Supplementary Information (SI) for Journal of Materials Chemistry C.

Supporting Information

Nanoporous and Morphology-transforming g-CNNPs for Trace-level detection of Mefenamic Acid in Urine samples and *in vitro* Protein denaturation inhibition

Anusree S. Gangadharan,[a] Daniel T. Thangadurai,[a]* Nandhakumar Manjubaashini[b] and Devaraj Nataraj[c]

[a]*Department of Chemistry and Centre for Nanoscience and Technology, KPR Institute of Engineering and Technology, Coimbatore 641407, Tamilnadu, India.*

[b]*National Centre for Nano Science and Technology, University of Madras, Chennai,600025, Tamilnadu, India.*

[c]*Department of Physics, Bharathiar University, Coimbatore 641046, Tamilnadu, India.*

**Corresponding author: Tel.: +914222635600; Email: danielthangadurai.t@kpriet.ac.in*

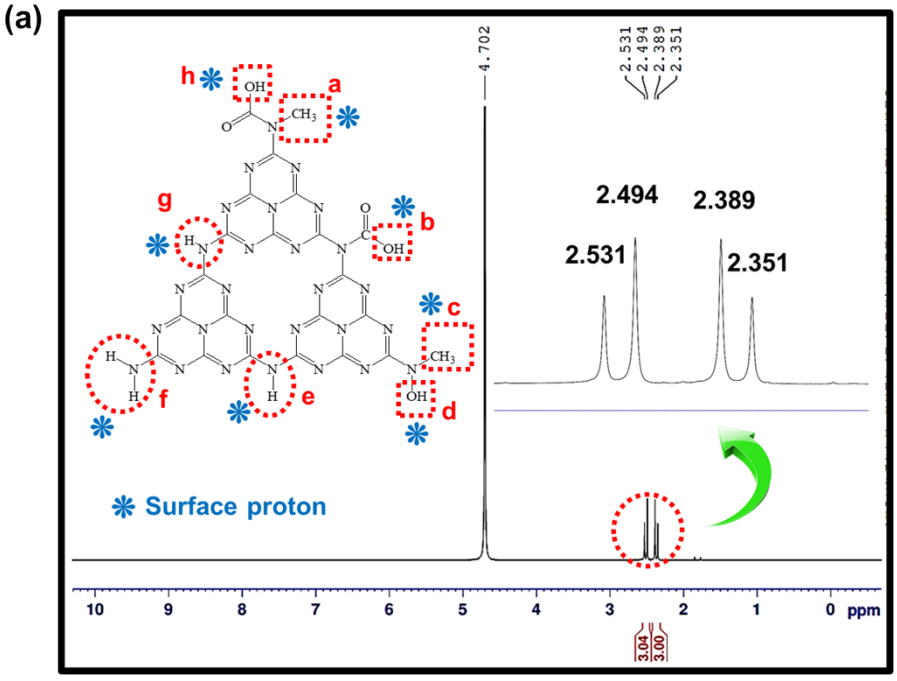

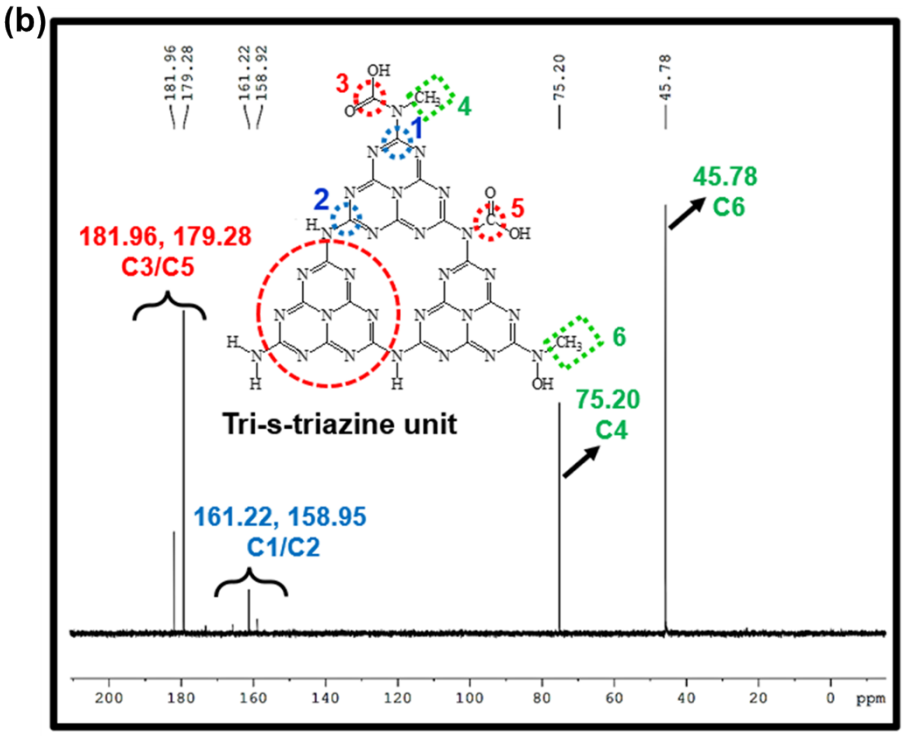

Figure S1. (a) ^{1}H NMR , and (b)^{13}C NMR spectrum of g-CNNPs.

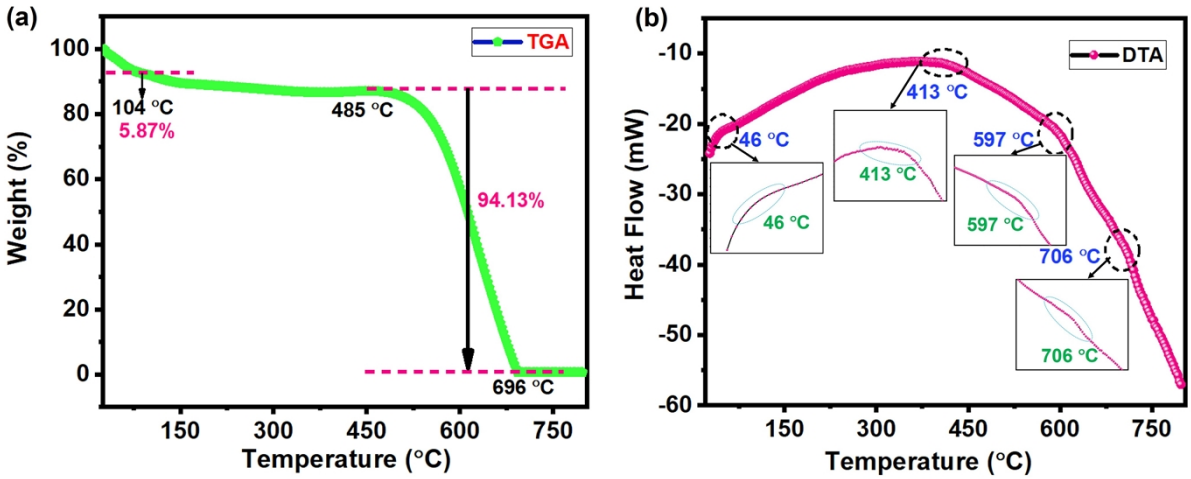

Figure S2. (a) TGA, and (b) DTA analysis of g-CNNPs.

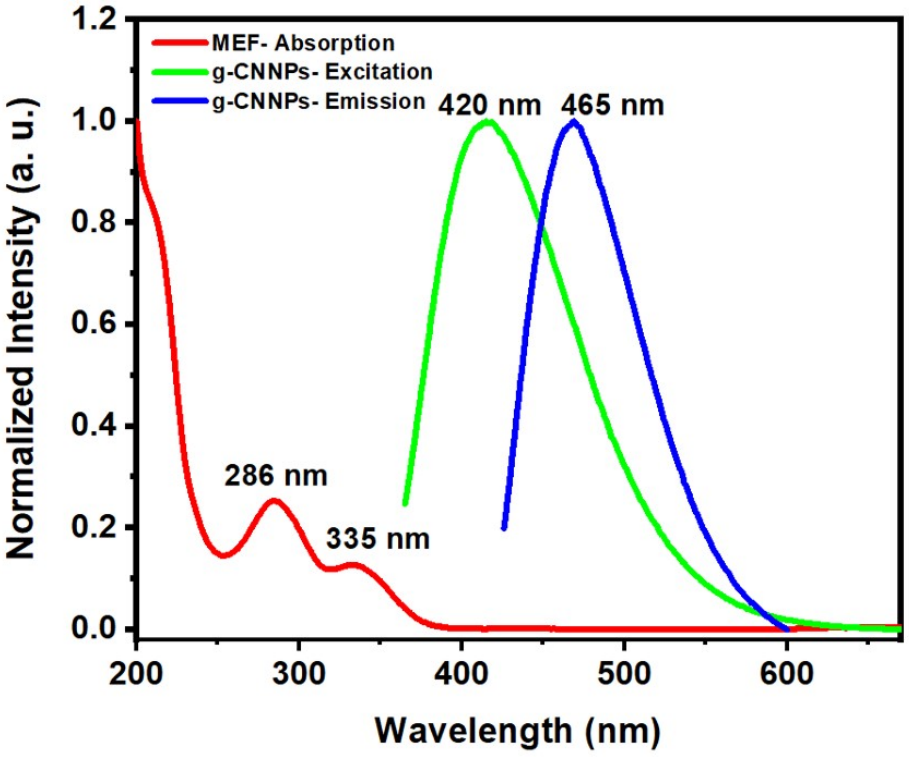

Figure S3. Normalized UV-visible absorption spectra of MEF, and PL excitation and emission spectra of g-CNNPs (λ_{ex}; 420 nm, slit width; 5 nm).

Binding constant, LoD, and LoQ calculations

From the fluorescence titration experiments, the binding strength between g-CNNPs and FPN was calculated by using the following equation.

$$\log[F\text{-}F_0/F_0] = \log K_a + n\log[Q] \qquad \text{(eq.S1)}$$

Where "F" is the fluorescence intensity after the addition of FPN and "F_0" is the initial fluorescence intensity of g-CNNPs. "K_a" is the binding constant, "n" is the number of binding sites, and "Q" is the concentration of guest, [MEF]. The K_a and 'n' can be estimated from the intercept and slope obtained by plotting $\log[F\text{-}F_0/F_0]$ against log[Q]. The fluorescence intensity was measured with the addition of MEF in different concentrations (Q) to the solution of g-CNNPs and they are labeled as 'F'. From the plot mentioned, the slope

and intercept are calculated. LoD and LoQ are obtained from the slope and intercept (eq. S2 and eq. S3, respectively).

$$LoD = [3\times(\text{intercept/slope})] \quad \text{(eq.S2)}$$

$$LoQ = [10\times(\text{intercept/slope})] \quad \text{(eq.S3)}$$

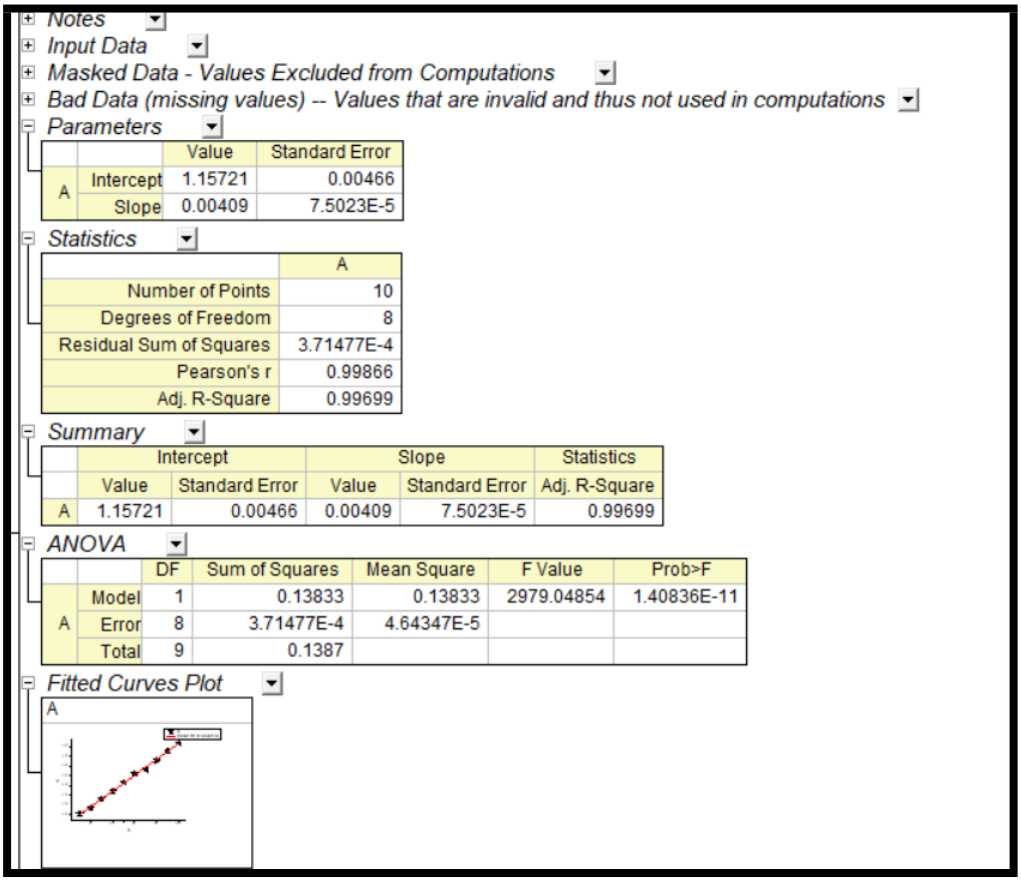

Figure S4. Datasheet of fluorescence emission intensity changes of g-CNNPs after the gradual addition of MEF and the limit of detection (LoD) is calculated via linear fit.

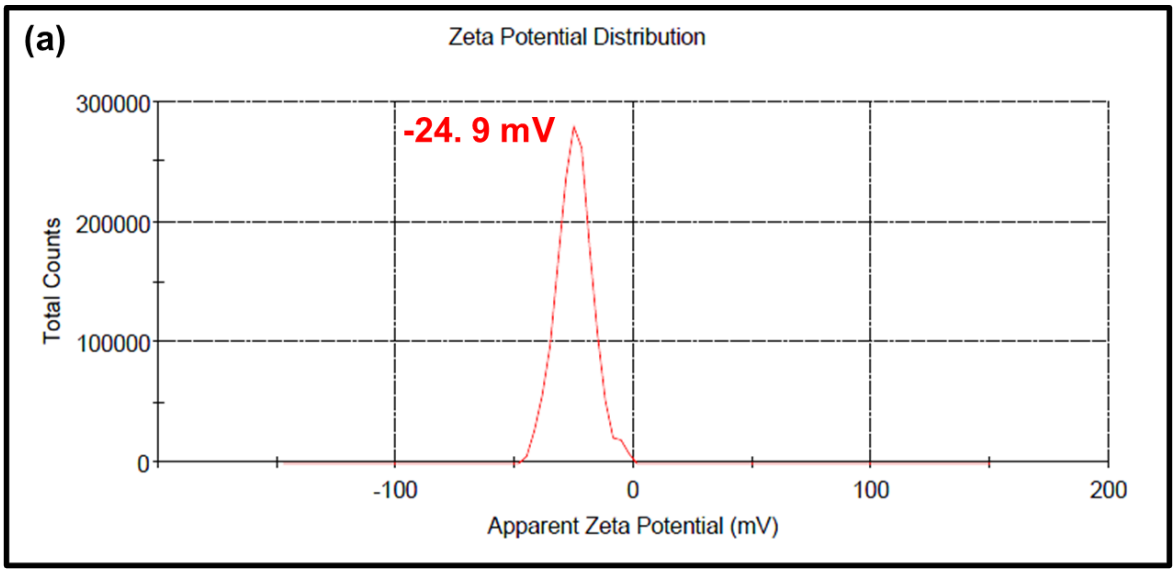
(a)
Zeta Potential Distribution
-24. 9 mV
300000
200000
100000
0
Total Counts
-100
0
100
200
Apparent Zeta Potential (mV)

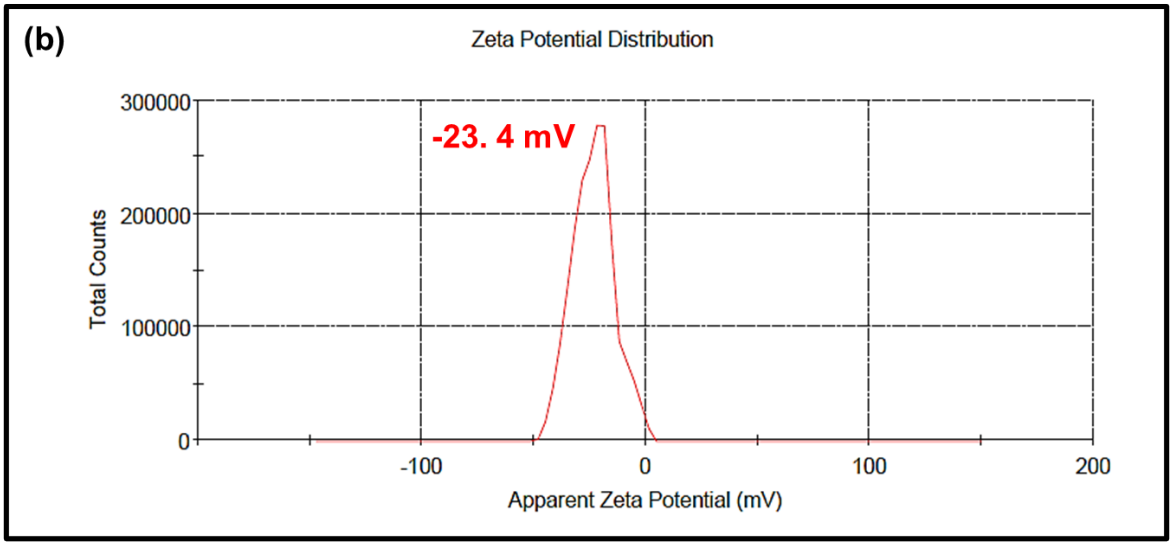
(b)
Zeta Potential Distribution
-23. 4 mV
300000
200000
100000
0
Total Counts
-100
0
100
200
Apparent Zeta Potential (mV)

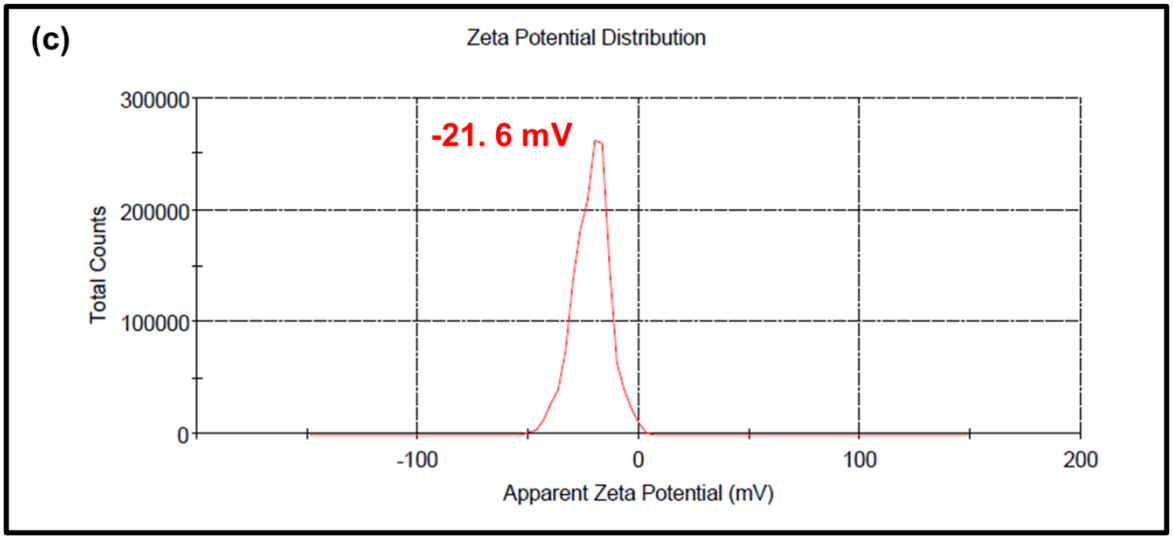
(c)
Zeta Potential Distribution
-21. 6 mV
300000
200000
100000
0
Total Counts
-100
0
100
200
Apparent Zeta Potential (mV)

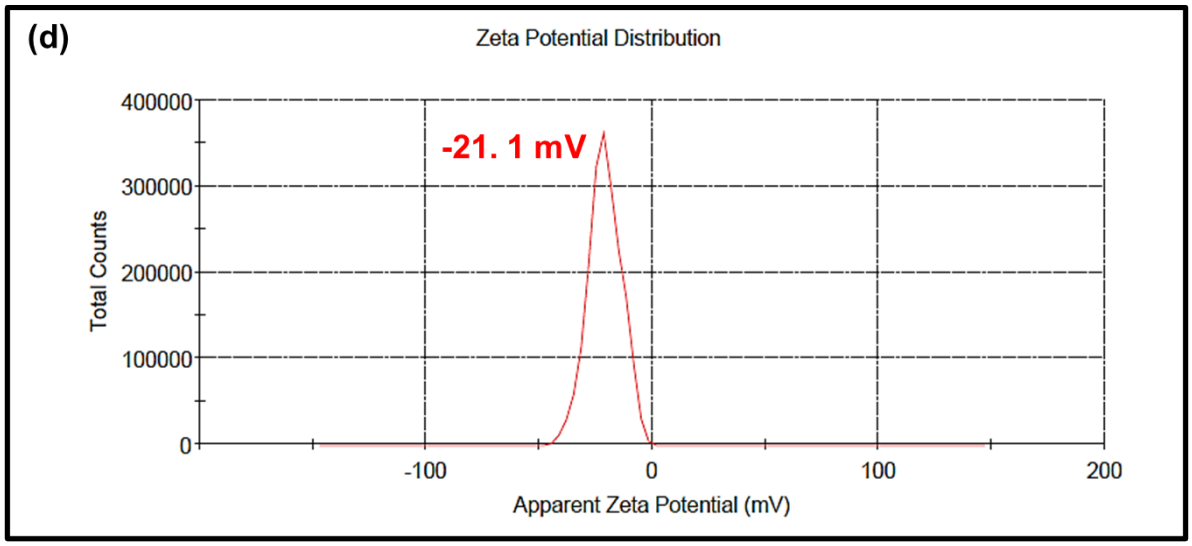

Figure S5: Zeta potential measurements of (a) g-CNNPs with the addition of MEF in different concentrations ((b) 0.25; (c) 0.5; and (d) 0.75 eq.).

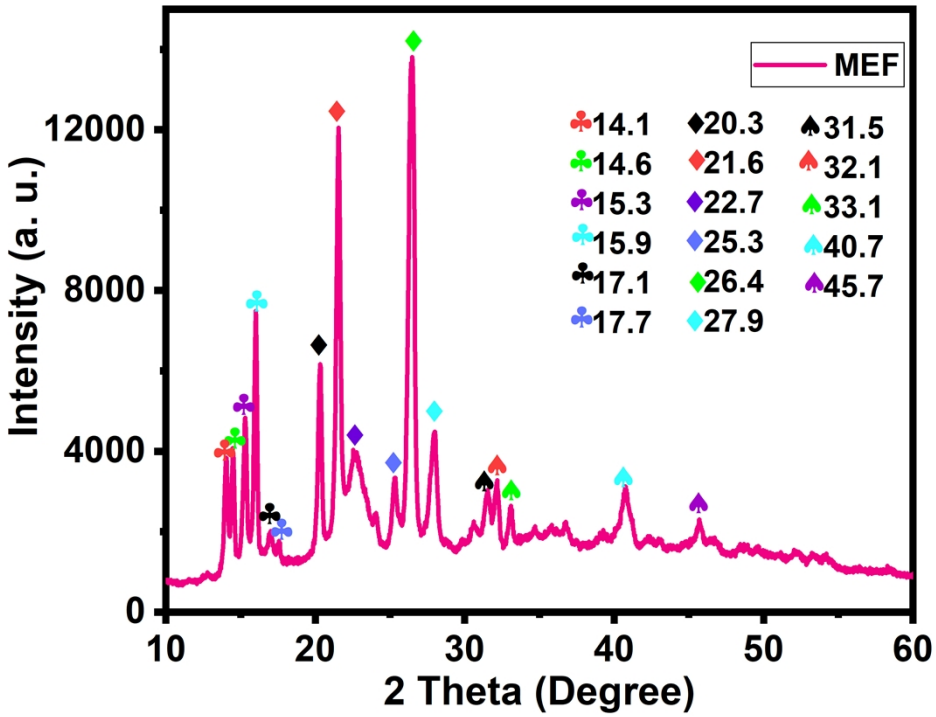

Figure S6. XRD pattern of mefenamic acid (MEF).

Table S1. The 2θ (λ=0.154 nm), plane, and interplanar distances (d_{hkl}) of MEF were obtained from XRD data.

Sl. No	Peak position (2θ /degree)	Plane	d (nm)
1	14.1	(010)	0.63
2	14.6	(110)	0.61
3	15.3	(011)	0.58
4	15.9	(101)	0.56
5	17.1	(111)	0.52
6	17.7	(021)	0.50
7	20.3	(120)	0.44
8	21.6	(130)	0.41
9	22.7	(131)	0.39
10	25.3	(040)	0.35
11	26.4	(141)	0.34
12	27.9	(150)	0.32
13	31.5	(002)	0.28
14	32.1	(221)	0.28
15	33.1	(222)	0.27
16	40.7	(240)	0.22
17	45.7	(260)	0.20

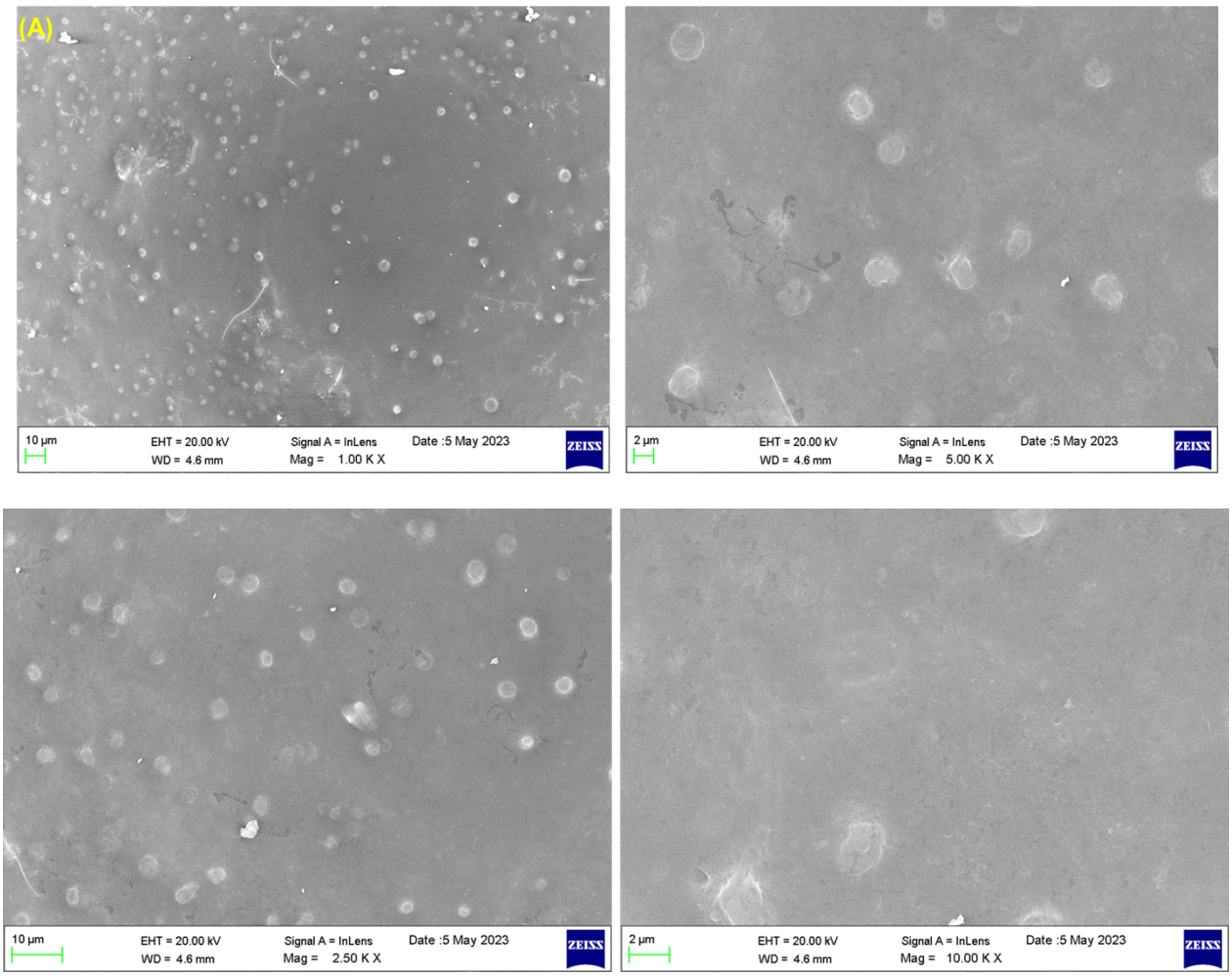
(A)
10 µm
EHT = 20.00 kV
WD = 4.6 mm
Signal A = InLens
Mag = 1.00 K X
Date :5 May 2023
ZEISS
2 µm
EHT = 20.00 kV
WD = 4.6 mm
Signal A = InLens
Mag = 5.00 K X
Date :5 May 2023
ZEISS
10 µm
EHT = 20.00 kV
WD = 4.6 mm
Signal A = InLens
Mag = 2.50 K X
Date :5 May 2023
ZEISS
2 µm
EHT = 20.00 kV
WD = 4.6 mm
Signal A = InLens
Mag = 10.00 K X
Date :5 May 2023
ZEISS

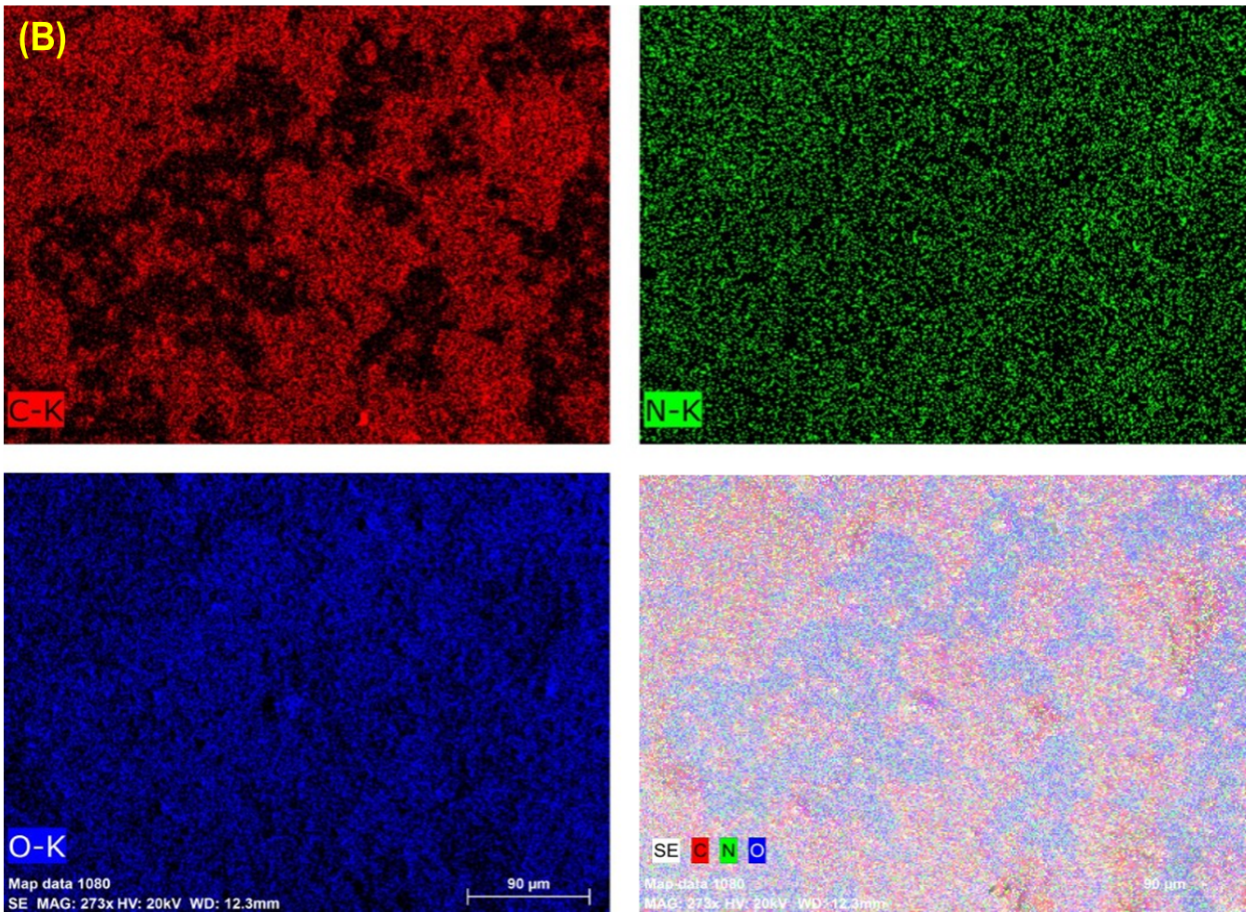

Figure S7. (A) FESEM images of g-CNNPs, and (B) Elemental mapping (C, N, O, and all together) of g-CNNPs.

Table S2. Percentage composition table of N, O, and C from EDS analysis of g-CNNPs.

Spectrum: BM 2643

El	AN	Series	unn. C [wt.%]	norm. C [wt.%]	Atom. C [at.%]	Error (1 Sigma) [wt.%]
O	8	K-series	75.30	75.30	70.03	9.35
C	6	K-series	21.14	21.14	26.19	3.24
N	7	K-series	3.56	3.56	3.78	1.01
		Total:	100.00	100.00	100.00	

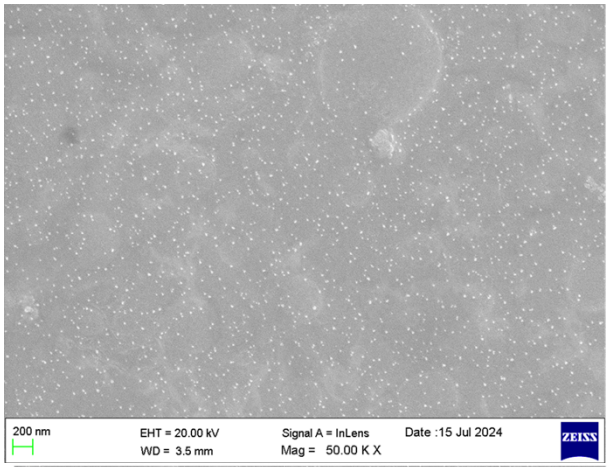
200 nm
EHT = 20.00 kV
WD = 3.5 mm
Signal A = InLens
Mag = 50.00 K X
Date :15 Jul 2024
ZEISS

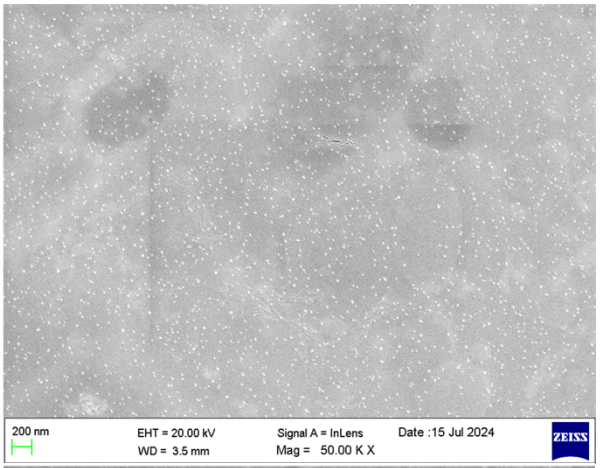
200 nm
EHT = 20.00 kV
WD = 3.5 mm
Signal A = InLens
Mag = 50.00 K X
Date :15 Jul 2024
ZEISS

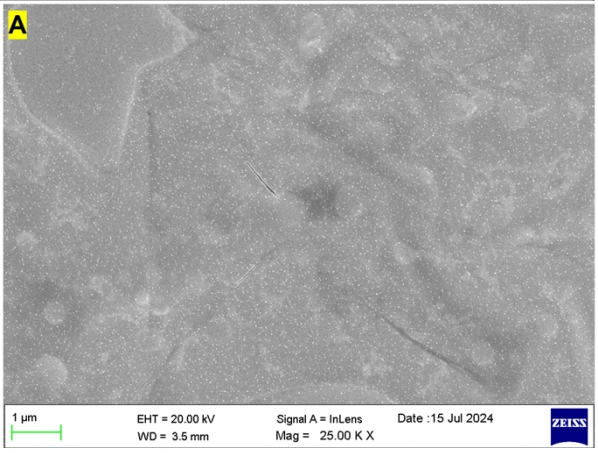
A
1 µm
EHT = 20.00 kV
WD = 3.5 mm
Signal A = InLens
Mag = 25.00 K X
Date :15 Jul 2024
ZEISS

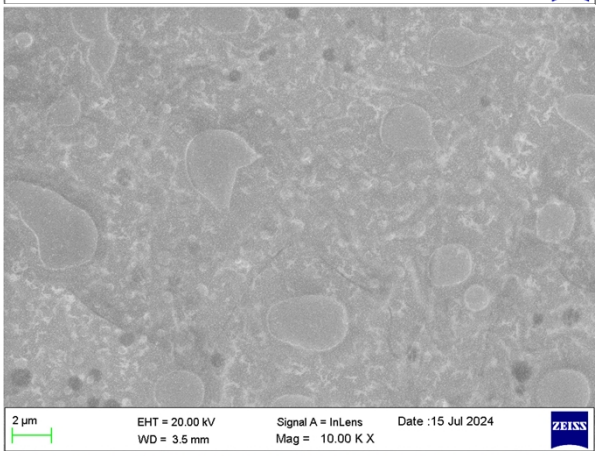
2 µm
EHT = 20.00 kV
WD = 3.5 mm
Signal A = InLens
Mag = 10.00 K X
Date :15 Jul 2024
ZEISS

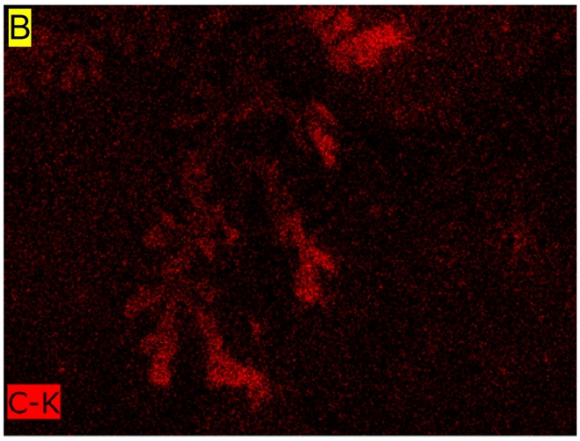
B
C-K

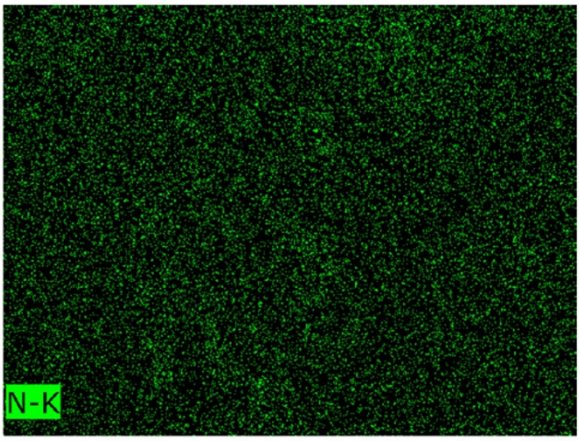
N-K

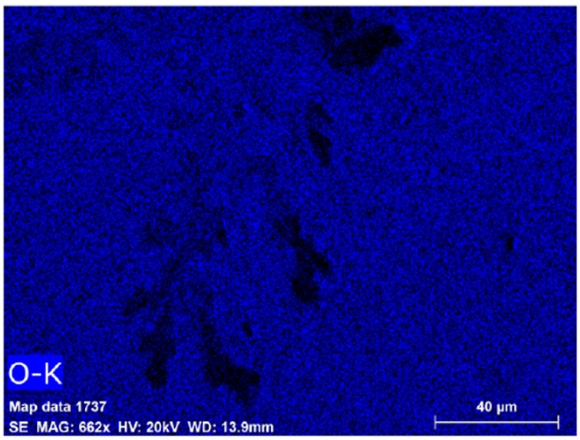
O-K
Map data 1737
SE MAG: 662x HV: 20kV WD: 13.9mm
40 µm

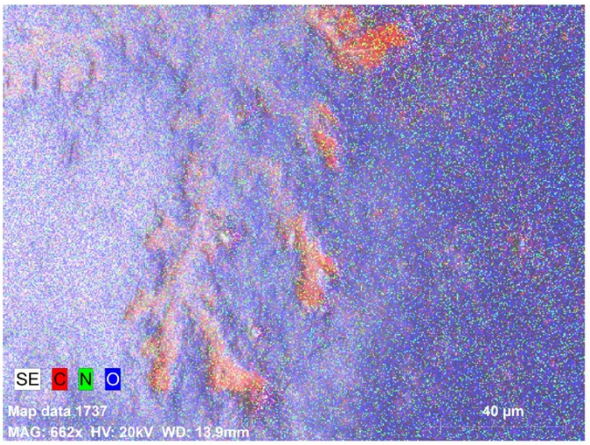
SE C N O
Map data 1737
MAG: 662x HV: 20kV WD: 13.9mm
40 µm

Figure S8. (A) FESEM images of g-CNNPs●MEF, and (B) Elemental mapping (C, N, O, and all together) of g-CNNPs●MEF.

Table S3. Percentage composition table of N, O, and C from EDS analysis of g-CNNPs●MEF.

Spectrum: BM 4416

El	AN	Series	unn. C [wt.%]	norm. C [wt.%]	Atom. C [at.%]	Error (1 Sigma) [wt.%]
O	8	K-series	70.79	70.79	64.79	8.77
C	6	K-series	26.92	26.92	32.81	3.83
N	7	K-series	2.29	2.29	2.39	0.76
		Total:	100.00	100.00	100.00	

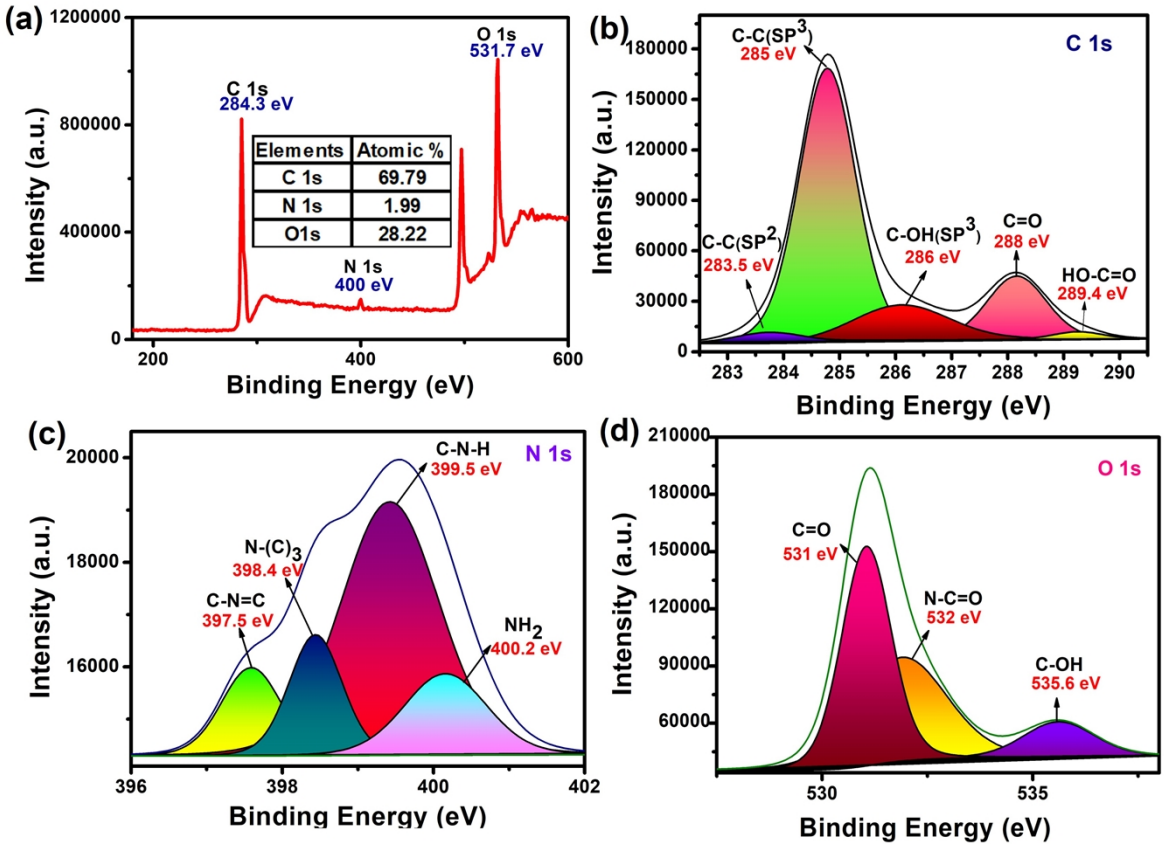

Figure S9. (a) XPS survey spectra of g-CNNPs and high-resolution peak fitting spectra of C 1s (b), N 1s (c), and O 1s (d).

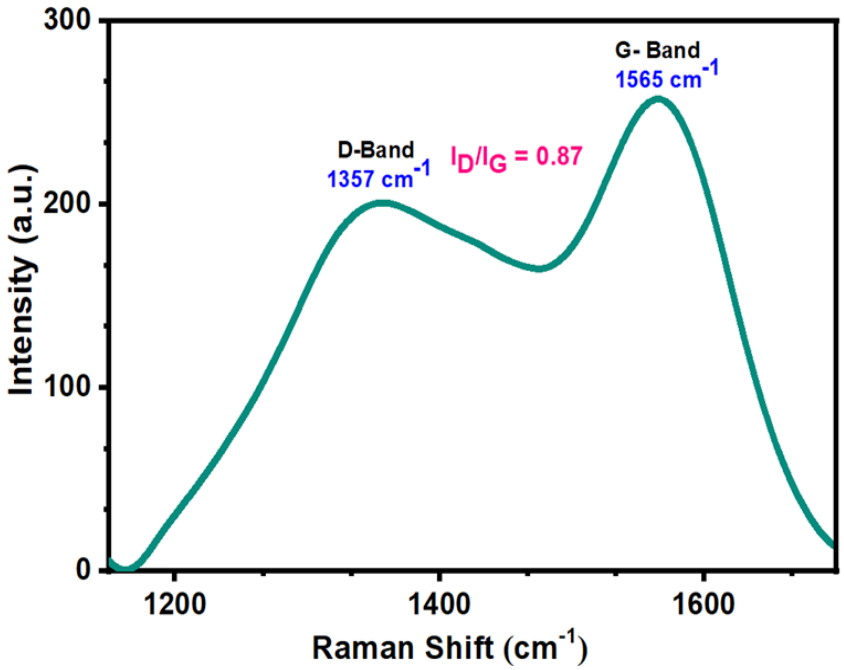

Figure S10. Raman spectra of g-CNNPs.

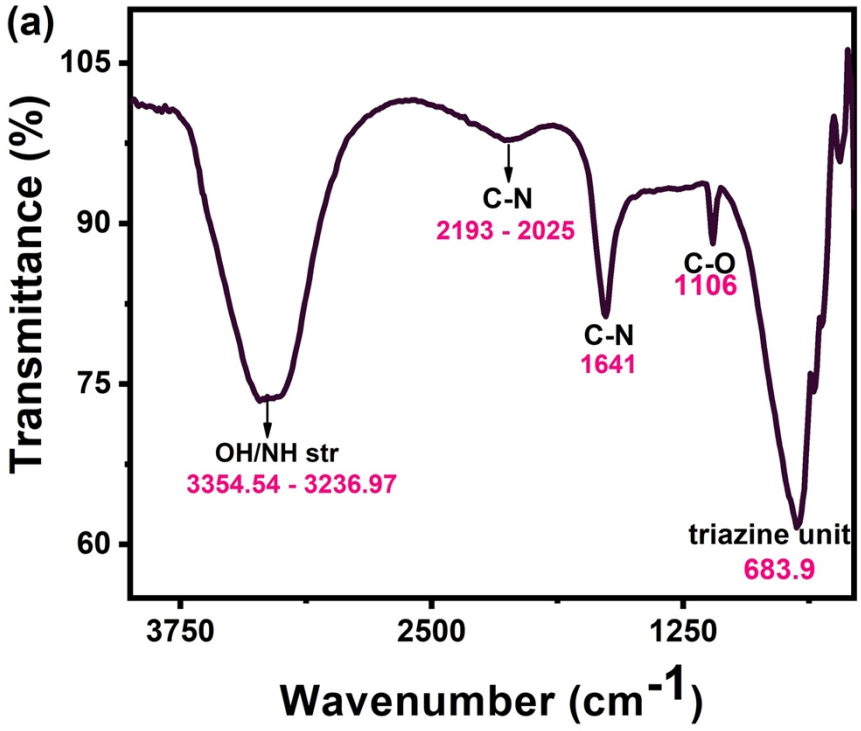

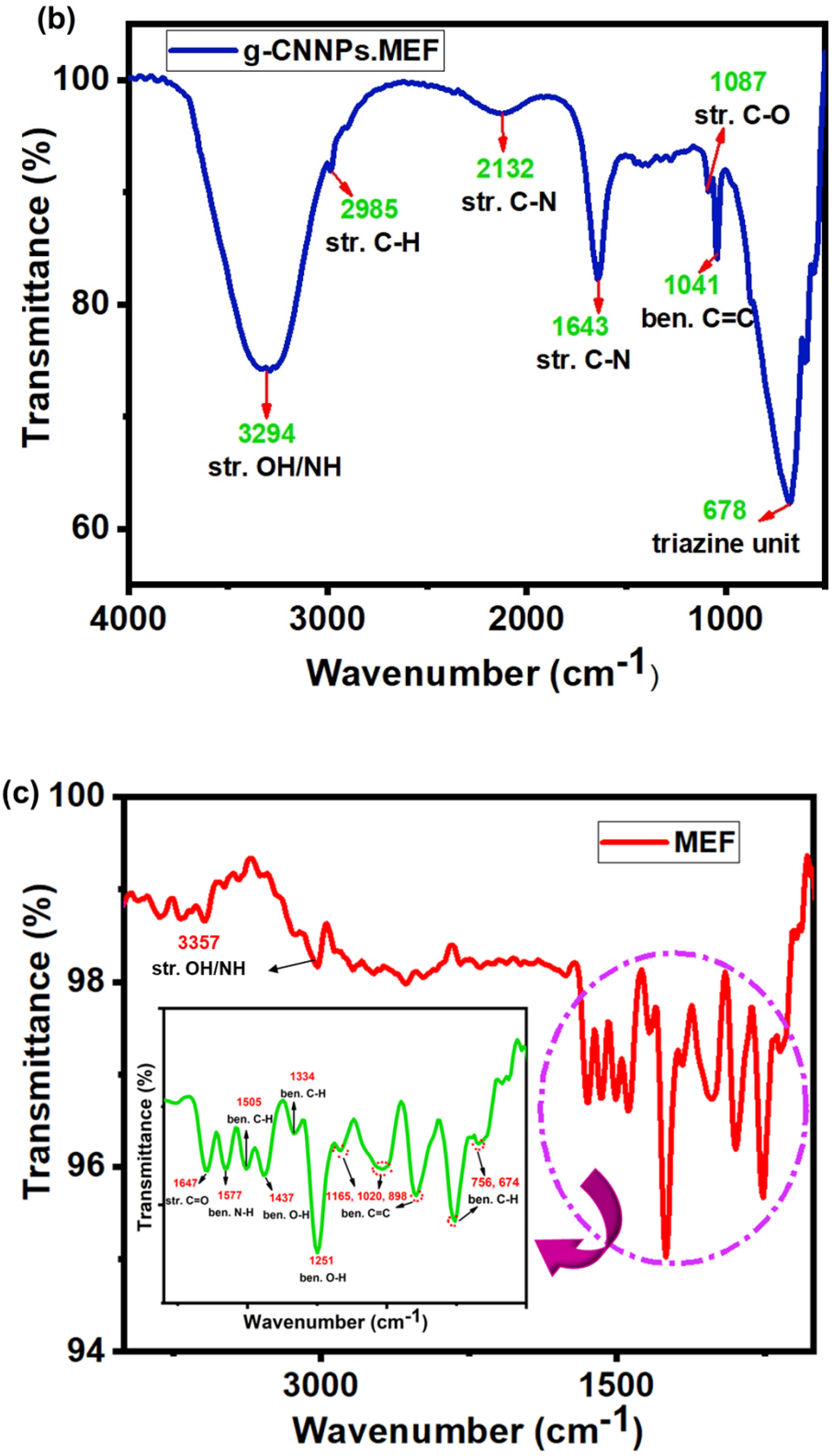

Figure S11. FT-IR spectra of g-CNNPs (a), g-CNNPs●MEF (b), and MEF (c).

Table S4. FT-IR spectrum of MEF identification.

Sl. No	Functional groups	Mode of vibration	Observed frequency (cm^{-1})
1	OH/NH	stretching	~3357
2	C=O	stretching	~1647
3	N-H	bending	~1577
4	C-H	bending	~1505, ~1334, ~756, ~674
5	O-H	bending	~1437, ~1251
6	C=C	bending	~1165, ~1020, ~898

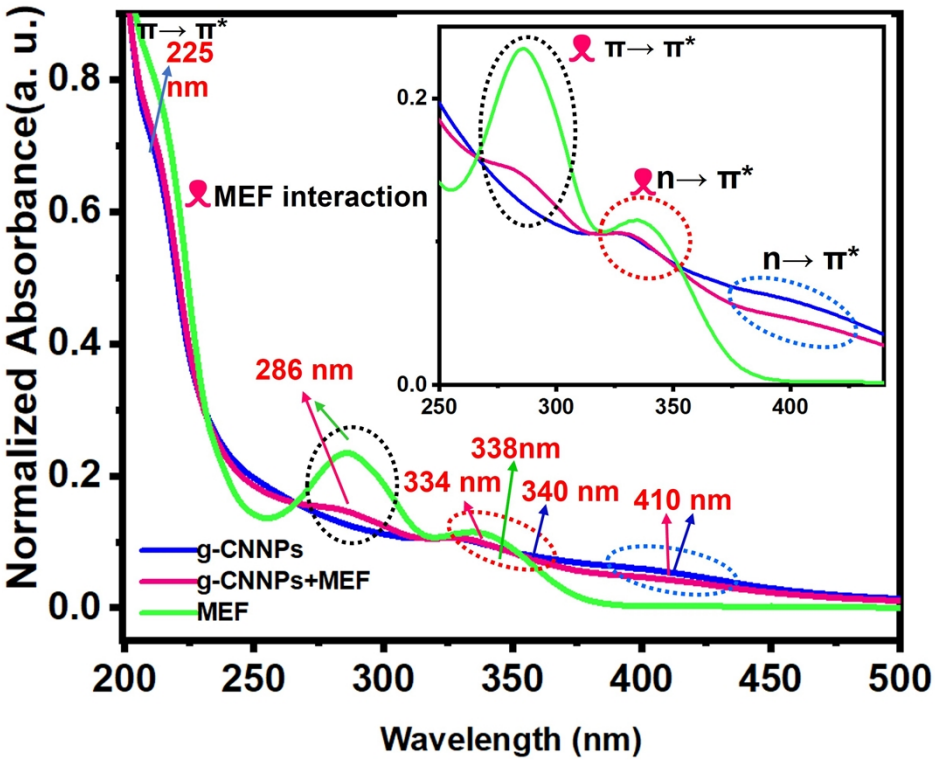

Figure S12. The Normalized UV-Vis spectra of isolated g-CNNPs, MEF, and g-CNNPs•MEF.

Contact angle analysis:

To measure the contact angle, a g-CNNPs pellet was prepared a by compressing a known amount of powder into a circular disc shape. Placed the resulting pellet on a flat surface and ensure it is securely fixed. Dispense a small droplet of the test water onto the surface of the pellet using a micro-syringe. Capture an image of the droplet on the pellet surface using a contact angle goniometer. The contact angle was measured by analyzing the captured images typically using software that calculates the angle between the droplet and the pellet surface.

Table S5. Comparison of MEF detection by various materials and techniques reported so far.

Sl. No	Material	Linier Range	LoD	Sensing Method	Real Sample Analysis	References
1	CV/CPE	0.01 to 470 µM	0.0023 µM	electrochemical	human blood, and pharmaceutical samples	[13]
2	SWCNTs/GCE	0.1 to 35 µM	14.3 nM	electrochemical	human urine	[33]
3	NiO-SWCNTs/ DDPM/CPE	1.0 to 600 µM	0.5 µM	electrochemical	tablet, injection, and pharmaceutical serum	[34]
4	CVO/RGO/GCE	0.001-to 425 µM	0.0079 µM	electrochemical	human blood serum and urine	[35]
5	FCDs@SiO_2-TPA	1.0 to 8 µM	197 nM	fluorescence	water, and cow urine	[36]
6	DMO/CNF/GCE	0.01 to 741 µM	0.009 µM	electrochemical	human blood and tablet	[37]
7	mpg-C_3N_4/ PANI/CdO	0.2 to 400 µM	0.045 µM	electrochemical	human serum	[38]

8	Co_3O_4NPs	1 to 500 µM	0.3 µM	electrochemical	-	[39]
9	Zn-Fe_2O_4@ Ni-AlLDH	50 to 100 nM	6.3 nM	electrochemical	tablet, human plasma, urine, and pharmaceutical wastewater	[40]
10	g-CNNPs	10 to 100 nM	3.4 nM	fluorescence	humane urine	This Work